Journal of Engineering Science and Technology
Vol. 13, No. 6 (2018) 1751 - 1763

DIRECT POWER CONTROL OF THREE-PHASE PWM RECTIFIER BASED ON NEW SWITCHING TABLE

TARIK MOHAMMED CHIKOUCHE*, KADA HARTANI

Electrotechnical Engineering Laboratory, Faculty of Technology,
Tahar Moulay University of Saida, BP 138, En-Nasr, Saida 20000, Algeria
*Corresponding Author: tchikouche@yahoo.fr

Abstract

This paper proposes a new switching table to improve the direct power control of three-phase PWM rectifier and achieve better performance in terms of power ripple reduction and dynamic response. This approach, which is based on the change of active and reactive power, can select the optimal rectifier voltage to overcome the power ripple and eliminate the harmonic current, and therefore reduce the total harmonic distortion of the line current and improve the power factor. To test this approach, a simulation platform using Matlab/Simulink was built. Simulations have been made to verify the effectiveness of the presented approach.

Keywords: Direct power control, Power ripple, PWM rectifier, Switching table, Unity power factor.

1. Introduction

In recent years, PWM rectifiers have been widely used in a variety of industrial applications due to their advanced qualities, such as absorption of sinusoidal current with low harmonic distortion and the possibility of operation with a power factor unity possibility of regeneration energy and DC-bus voltage control over a large range [1-3]. Three-phase PWM rectifiers have been progressively employed, such as in adjustable speed drives, HVDC systems, active power filter, wind, photovoltaic and other renewable power generation systems [1, 3-5].

Many control strategies have been proposed for these PWM rectifiers. They can be classified into two categories [6-8], voltage oriented control (VOC) analogue to the vector control of electrical machines [9-11], and direct power control (DPC) analogue to the direct torque control of electrical machines [12].

Nomenclatures

C, R_L	DC-link capacitor and load resistance
i_a, i_b, i_c	Three-phase power-source currents, amperes.
L, R	Inductance and resistance of smoothing inductor
S_a, S_b, S_c	Switching states of the converter
S_p, S_q	Digital signal of instantaneous errors of active and reactive power
V_M	Amplitude of the AC voltage, volts.
v_a, v_b, v_c	Three-phase power-source voltages, volts
v_{ra}, v_{rb}, v_{rc}	Terminal voltages of the PWM rectifier, volts.

Greek Symbols

α, β	Stationary frame
ε_p, ε_q	Errors of active and reactive power
θ_n	Voltage vector position, deg.

Abbreviations

DPC	Direct Power Control
HVDC	High Voltage Direct Current
PWM	Pulse With Modulation
VOC	Voltage Oriented Control
VSR	Voltage Source Rectifier

The classical control of PWM rectifier is VOC, which decomposes the grid currents into active and reactive power components and regulate them separately [8]. Although good steady state performance and dynamic responses are obtained using VOC, its performance relies heavily on the internal current control and PI tuning [13]. Compared to VOC, the DPC can achieve very quick response with a simple structure by selecting a voltage vector from predefined switching table. Concerning the VOC it is not accurate for it gives large power ripples [14, 15].

In the conventional DPC [16], the active and reactive power are estimated using grid voltage and current measurements based on instantaneous power theory [17]. The hysteresis band control technique is used to compare instantaneous errors of active and reactive power. The output of the two-hysteresis controller and the position of the voltage vector constitute the inputs of the switching table, which imposes the switching state of the PWM rectifier [18-20].

The switching table has a very important role in the performance of the direct power control [20]. However, the use of only one voltage vector in the conventional switching table during one control period leads to high power ripples. The conventional switching table illustrated in [21], demonstrates that it is not satisfactory in the controlling of the active and reactive power. As results, some authors have revised the conventional switching table to achieve output regulation subspaces [22, 23] to select the desired voltage vectors.

In order to achieve better performance of DPC, a new switching table is proposed in this paper, based on the analysis of the change in active and reactive power, to select the optimal rectifier voltage. The aim of this method is also to eliminate the harmonic current and therefore reduce the total harmonic distortion of the line current and improve the power factor.

The paper is organized as follows: In Section 2, a model of the three-phase PWM rectifier is presented. In Section 3, a detailed study of DPC with a new switching table is carried out based on the analysis of the instantaneous active and reactive power, including steady state performance, dynamic response and robustness against external load disturbance. Simulation and discussion of the Simulink waveforms are presented in Section 4. In the end, Section 5 there is a comprehensive conclusion.

2. Model of the PWM rectifier

The topology of three-phase bidirectional voltage-source PWM rectifier (VSR) is shown in Fig. 1. The VSR is connected to the three-phase ac source via smoothing L and internal resistance R. It is assumed that a purely resistive load R_L is connected to the dc-link capacitor C [24].

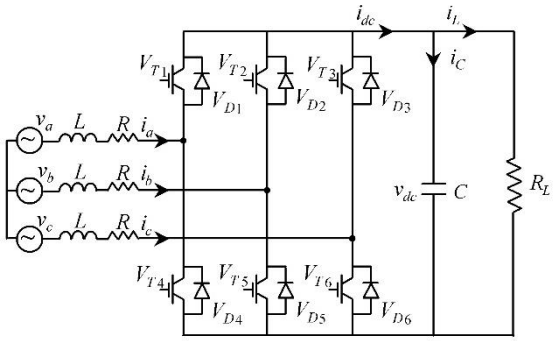

Fig. 1. Topology of three-phase PWM rectifier.

The model of the PWM rectifier can be expressed in (a,b,c) the frame as:

$$\begin{bmatrix} v_a \\ v_b \\ v_c \end{bmatrix} = R\begin{bmatrix} i_a \\ i_b \\ i_c \end{bmatrix} + L\frac{d}{dt}\begin{bmatrix} i_a \\ i_b \\ i_c \end{bmatrix} + \begin{bmatrix} v_{ra} \\ v_{rb} \\ v_{rc} \end{bmatrix} \tag{1}$$

$$c\frac{dv_{dc}}{dt} = S_a i_a + S_b i_b + S_c i_c \tag{2}$$

The phase voltage at the poles of the converter is equal to:

$$\begin{bmatrix} v_{ra} \\ v_{rb} \\ v_{rc} \end{bmatrix} = \frac{v_{dc}}{3}\begin{bmatrix} 2 & -1 & -1 \\ -1 & 2 & -1 \\ -1 & -1 & 2 \end{bmatrix}\begin{bmatrix} S_a \\ S_b \\ S_c \end{bmatrix} \tag{3}$$

The instantaneous active power and reactive power at the grid side can be calculated from grid voltage and current as [21, 25]:

$$\begin{cases} p = v_a i_a + v_b i_b + v_c i_c \\ q = \dfrac{1}{\sqrt{3}}\left[(v_b - v_c) i_a + (v_c - v_a) i_b + (v_a - v_b) i_c\right] \end{cases} \tag{4}$$

From the power model of PWM rectifier, we can know that different switching states have different influences on the active and reactive power. It is possible to select optimal switching states to adjust active and reactive power.

3. Proposed DPC with new switching table

3.1. Principle of the DPC

The direct power control (DPC) technique is based on the direct control of the active and reactive power of PWM rectifier. As shown in Fig. 2, the output of the two hysteresis controllers, which is presented, constitute the inputs of the proposed switching table which selects the optimal switching states of PWM rectifier [12, 17].

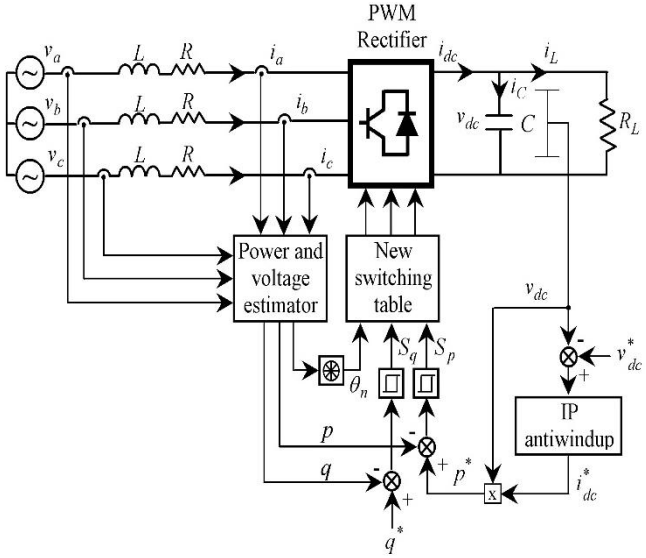

Fig. 2. Proposed DPC configuration of three-phase PWM rectifier.

The instantaneous values of active p and reactive q power are estimated in Eq. (4). The active power reference is obtained from the voltage controller of the DC bus. However, the reactive power reference is set to zero to get unity power factor [26, 27].

The *Sp* and *Sq* can show whether we should increase or reduce (decrease) the active or reactive power. The power model of PWM rectifier is given as [28]:

$$\begin{cases} L\dfrac{dp}{dt} = -R_p - \omega L_q - \left(v_\alpha v_{r\alpha} + v_\beta v_{r\beta}\right) + \left(v_\alpha^2 + v_\beta^2\right) \\ L\dfrac{dq}{dt} = -R_q + \omega L_p - \left(v_\alpha v_{r\alpha} - v_\beta v_{r\beta}\right) \end{cases} \tag{5}$$

From the power model of PWM rectifier, we can know that different switching states have different influences on the active and reactive power. It is possible to select the proper switching states to adjust the active and reactive power. The phase of the power-source voltage vector is converted to the digitized signal θ_n. For this purpose, the stationary coordinates are divided into 12 sectors, as shown in Fig. 3, and the sectors can be numerically expressed as:

$$(n-2)\frac{\pi}{6} \le \theta_n \le (n-1)\frac{\pi}{6} \qquad n = 1,2,\ldots,12 \tag{6}$$

3.2. Vector selection in the new switching table

The new switching table is formed from the output of the two-hysteresis controllers (S_p, S_q) and the angular position θ_n of the voltage vector. $S_P = 1$ stands for the need to increase the active power, while $S_P = 0$ denotes the need to decrease the active power. So is the case of the S_q. According to the inputs S_P and S_q, together with the sector information, the proper rectifier input voltage vector can be chosen and the corresponding switching stable will be sent to trigger the IGBTs of the main circuit.

Considering the value of R is small enough to be neglected, the instantaneous active and reactive power can be rewritten as:

$$\begin{cases} \dfrac{dp}{dt} = \dfrac{3}{2}\dfrac{V_M^2}{L} - \dfrac{V_M v_{dc}}{L}\cos\left[\omega t - \dfrac{\pi}{3}(k-1)\right] \\ \dfrac{dq}{dt} = -\dfrac{V_M v_{dc}}{L}\sin\left[\omega t - \dfrac{\pi}{3}(k-1)\right] + \omega p \end{cases} \tag{7}$$

where $k = 1,2,3,4,5,6$ corresponding to the no-zero selected voltage vector number shown in Fig. 3.

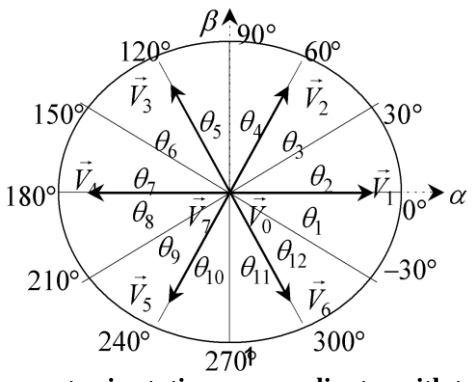

Fig. 3. Voltage vector in stationary coordinates with twelve sectors.

The variation of active power and reactive power versus grid voltage position for various rectifier voltage vectors are depicted in Fig. 4.

In order to achieve better performance of the system, the switching table should be synthesized based on the variation of active and reactive power for various

rectifier voltage vectors in each sector, as shown in Fig. 4. The signs of slope in active and reactive power are illustrated in Table 1 [29].

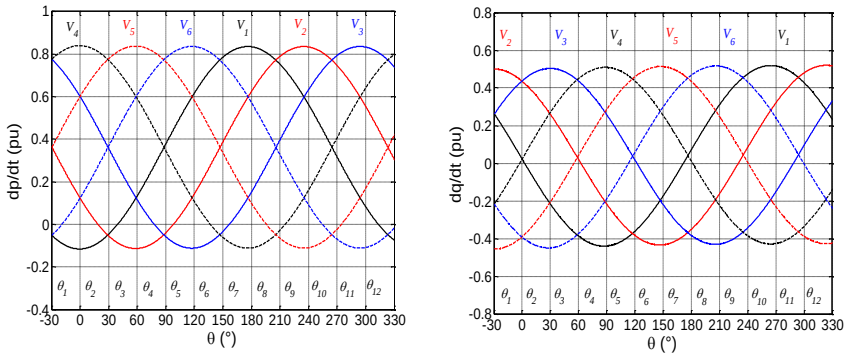

Fig. 4. Variation of active and reactive power for various rectifier voltage vectors.

Table 1. Signs of slope in active and reactive power for all sectors.

Sector	*dp/dt* *>0(S_p=1)*	*0<(S_p=0)*	*dp/dt* *>0(S_q=1)*	*0<(S_q=0)*
θ_1	V_2, V_3, V_4, V_5	V_1, V_6	V_1, V_2, V_3	V_4, V_5, V_6
θ_2	V_3, V_4, V_5, V_6	V_1, V_2	V_2, V_3, V_4	V_1, V_5, V_6
θ_3	V_3, V_4, V_5, V_6	V_1, V_2	V_2, V_3, V_4	V_1, V_5, V_6
θ_4	V_1, V_4, V_5, V_6	V_2, V_3	V_3, V_4, V_5	V_1, V_2, V_6
θ_5	V_1, V_4, V_5, V_6	V_2, V_3	V_3, V_4, V_5	V_1, V_2, V_6
θ_6	V_1, V_2, V_5, V_6	V_3, V_4	V_4, V_5, V_6	V_1, V_2, V_3
θ_7	V_1, V_2, V_5, V_6	V_3, V_4	V_4, V_5, V_6	V_1, V_2, V_3
θ_8	V_1, V_2, V_3, V_6	V_4, V_5	V_1, V_5, V_6	V_2, V_3, V_4
θ_9	V_1, V_2, V_3, V_6	V_4, V_5	V_1, V_5, V_6	V_2, V_3, V_4
θ_{10}	V_1, V_2, V_3, V_4	V_5, V_6	V_1, V_2, V_6	V_3, V_4, V_5
θ_{11}	V_1, V_2, V_3, V_4	V_4, V_5	V_1, V_2, V_6	V_3, V_4, V_5
θ_{12}	V_2, V_3, V_4, V_5	V_4, V_5	V_1, V_2, V_3	V_4, V_5, V_6

The new switching table for DPC of PWM rectifier can be summarized in Table 2.

Table 2. The new switching table for DPC of PWM rectifier.

Sp	Sq	θ_1	θ_2	θ_3	θ_4	θ_5	θ_6	θ_7	θ_8	θ_9	θ_{10}	θ_{11}	θ_{12}
1	*0*	V_4	V_5	V_5	V_6	V_6	V_1	V_1	V_2	V_2	V_3	V_3	V_4
	1	V_3	V_4	V_4	V_5	V_5	V_6	V_6	V_1	V_1	V_2	V_2	V_3
0	*0*	V_6	V_1	V_1	V_2	V_2	V_3	V_3	V_4	V_4	V_5	V_5	V_6
	1	V_1	V_2	V_2	V_3	V_3	V_4	V_4	V_5	V_5	V_6	V_6	V_1

3.3. Control of the DC-bus

The error between rectified voltage v_{dc} and reference v_{dc}^* is then fed to the anti-windup IP controller to obtain the current component command i_{dc}^* [24]. The product of rectifier voltage v_{dc} and the current reference obtained at the output of the anti-windup IP controller gives the active power reference.

The windup phenomenon can lead to instability of the system. Its cause is the integral term of the controllers. It is, therefore, necessary to stop the integration in the controllers during the period of saturation of the control. If the integral term is not limited, its value becomes very large, and it is necessary at the input of the controller a strongly negative error to return to the final value. For an IP controller, the integral term can be limited by using the algorithm (Table 3) represented by the block diagram in Fig. 5.

Table 3. IP anti-windup algorithm.

```
Err=Vdc_ref-Vdc;
Tintegral(n+1)=Tintegral(n)+ki*T*Err;
idc_ref=kp*(Tintegral(n+1)- Vdc);

if abs(idc_ref)>=abs(idc_max)
   idc_ref =sign(idc_ref)*idc_max;
   Tintegral(n+1)=idc_ref /kp+ Vdc;
End;
```

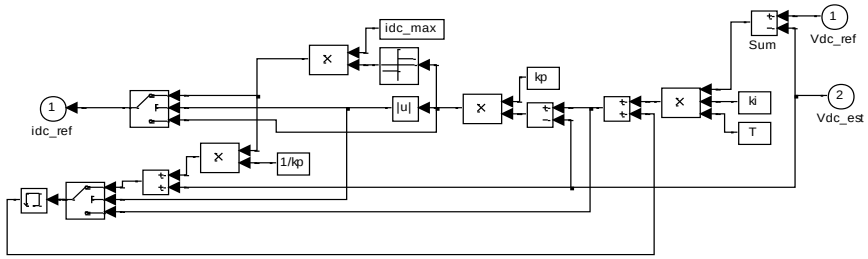

Fig. 5. The scheme of the anti-windup IP controller.

4. Results and Discussion

To confirm the effectiveness of the proposed DPC with new switching table, the simulation test is carried out on a two-level three-phase PWM rectifier. The main parameters of the simulation circuit are given in Table 4 [24].

Table 4. Rectifier parameters.

The input phase voltage : *V=125 V/F = 50 Hz*
The input inductance : *L= 37 Mh*
The input resistance : *R= 0.3* Ω
The output capacitor : C_{dc}*= 1100 µF*
The output voltage : v_{dc} *= 350 V*

In this simulation test we have imposed the reference of the DC bus voltage at 350V, and then introduced a perturbation characterized by a change in the load resistance between the instant $t = 0.3s$ and $t = 0.5s$.

Figure 6(a) shows the evolution of the DC bus voltage. We notice from this response that the voltage v_{dc} follows perfectly its reference. There is a satisfactory steady-state operation with no static error, which shows that the proposed analytical approach for the design of the IP regulator is rigorous, Fig. 6(b). The application of the disturbance affects the DC bus voltage with a weak drop on the order of 0.86%

for a brief period of 0.08 s. This means that the voltage IP regulator acts well in the rejection of this disturbance. To show the efficiency of the IP regulator, the normalized error of the DC bus voltage does not exceed 0.1% as it is shown in Fig. 6(c). The introduction of the perturbation characterized by a decrease in the load resistance applied at the instant $t = 0.3s$ in steady state causes an increase in the load current, which response instantaneously to this variation, Fig. 6(h). It can be seen that after the instant $t = 0.5s$, the current i_L is kept constant at its nominal value (0.7A).

The current response is practically instantaneous, as shown in Fig. 6(d), which represents the three currents at the input of the rectifier corresponding to the current operation. In the transient mode, these currents show a transient with a rapid increase when the load is applied, Fig. 6(e). Then they stabilize at an amplitude of 0.80A after the instant $t = 0.5s$, Fig. 6(f). We notice that these grid currents are sinusoidal which gives a low rate of harmonic distortion. Fig. 6(k) shows the harmonic spectrum of the response of the grid current i_a. It is noted that all the low render harmonics are well attenuated, which gives a rate of harmonic distortion (THD =0.96%). From Figs. 6(d)-(g), it can be seen that this current is purely sinusoidal. Fig. 6(i) shows that the grid current is in phase with the power-source voltages because the reactive power command q^* is set to zero, which gives a unity power factor.

The power response is illustrated in Fig. 6(j). The active power increases from 245 W to 490 W $t = 0.3s$ and then decreases to initial value at $t = 0.5s$. We can see that the response of this structure provides excellent performances. The proposed DPC with a new switching table adjusts well the active power in all sectors when the load power increases. It is clearly seen that in Fig. 6(j), the reactive power is kept at zero to achieve a unity power factor. From this figure, it can be found that the active power control and the reactive power control are independent of each other. The load resistance was changed stepwise in this test. It can be observed that the unity power factor operation is successfully achieved, even in this transient state. Notice that, after a short transient, the output voltage is maintained close to its reference value.

Finally, the simulation results show that the proposed DPC can achieve a decoupled control of active and reactive power when the load changes.

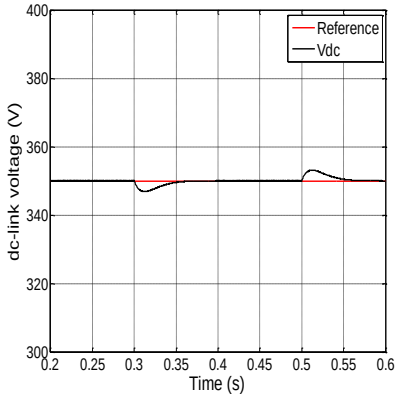

(a) DC output voltage.

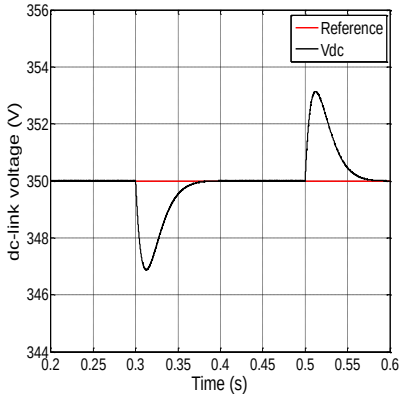

(b) Zoom of the DC output voltage.

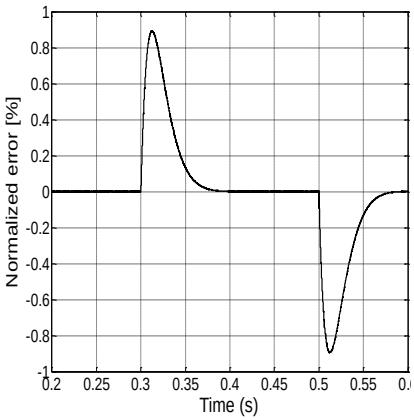

(c) Normalized error of the DC output voltage

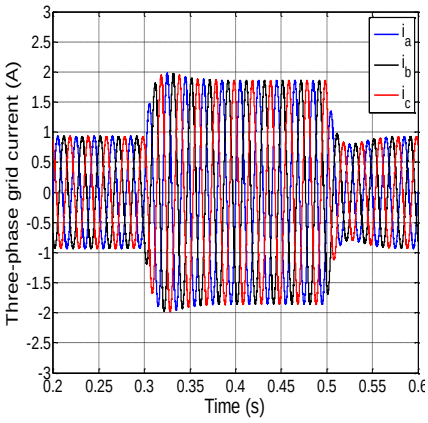

(d) Line current.

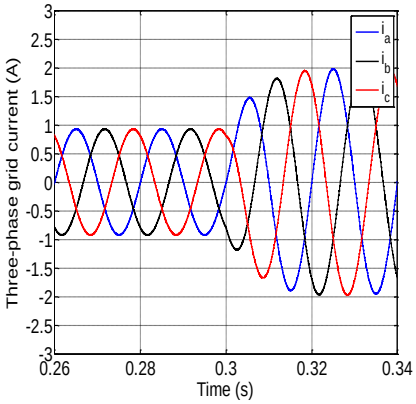

(e) Zoom of line current.

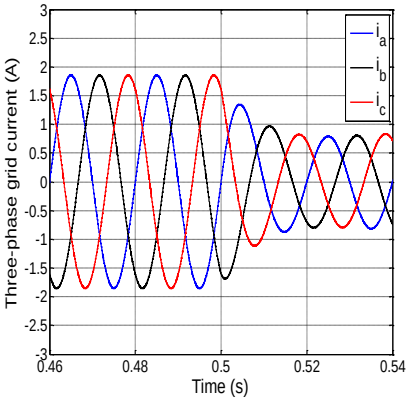

(e) Zoom of line current.

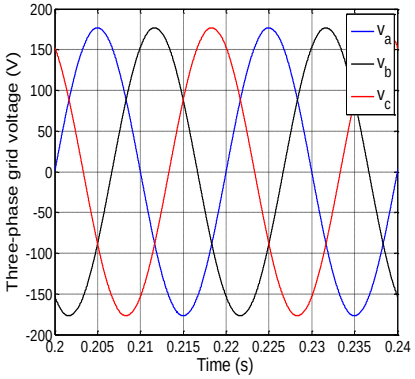

(g) Line voltage.

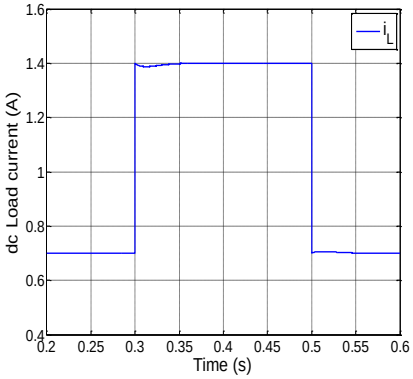

(h) Load current.

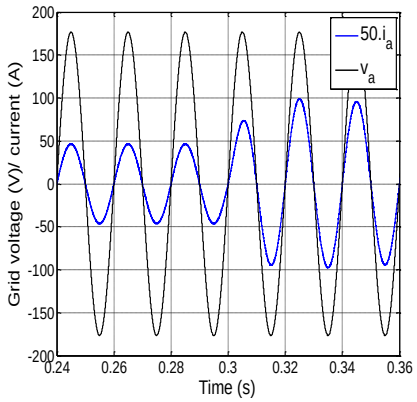

(i) Voltage and current waveforms of phase *a* .

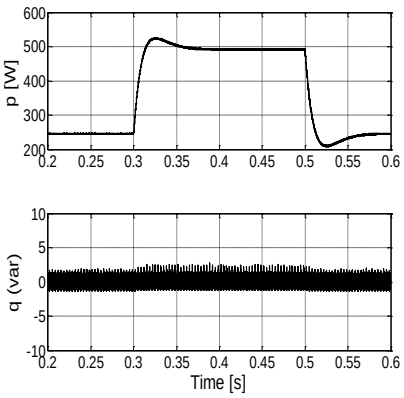

(j) Active power and reactive power.

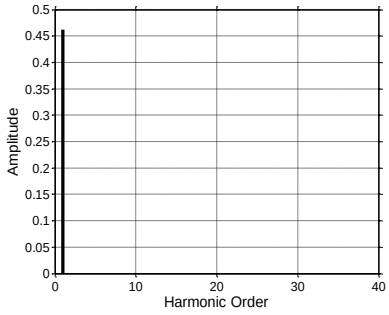

(k) Line current spectrum of phase *a* .

Fig. 6. Simulation results in steady state of the step change of load power for v_{dc} = *350 V* and *q* = 0 var (increase 50%)

5. Conclusions

Based on the analysis of the variation of instantaneous active and reactive power, a new switching table for direct power control of two-level three-phase PWM rectifier is obtained by correcting the active and reactive power at the same time. The simulation results show that instantaneous active and reactive power and DC-bus voltage follow their references with high precision and stability. The observed currents are in phase with the grid line voltages that provide a unity power factor. Compared to the conventional switching table, the proposed method can choose a more appropriate switching state by considering the change of the active and reactive power. A better steady state performance was achieved.

References

1. Rodríguez, J.R.; Dixon, J.W.; Espinoza, J.R.; Pontt, J.; and Lezana, P. (2005). PWM regenerative rectifiers: State of the art. *IEEE Transactions on Industrial Electronics*, 52(1), 5-22.

2. Aissa, O.; Moulahoum, S.; Kabache, N.; and Houassine, H. (2014). Fuzzy logic based direct power control for PWM three-phase rectifier. *Proceedings of the 22nd Mediterranean Conference in Control and Automation (MED)*. Palermo, Italy, 79-84.
3. Hashmi, M.U. (2012) *Design and development of upf rectifier in a microgrid environment*. Masters Thesis. Department of Energy Science and Engineering, Indian Institute of Technology Bombay, India.
4. Hang, L.; Liu, S.; Yan, G; Qu, B.; and Lu, Z.-y. (2011). An improved deadbeat scheme with fuzzy controller for the grid-side three-phase PWM boost rectifier. *IEEE Transactions on Power Electronics*, 26(4), 1184-1191.
5. Liutanakul, P.; Pierfederici, S.; and Meibodi-Tabar, F. (2008). Application of SMC with I/O feedback linearization to the control of the cascade controlled-rectifier/inverter-motor drive system with small dc-link capacitor. *IEEE Transactions on Power Electronics*, 23(5), 2489-2499.
6. Norniella, J.G.; Cano, J.M.; Orcajo, G.A.; Rojas, C.H.; Pedrayes, J.F.; Cabanas, M.F.; and Melero, M.G. (2010) Optimization of direct power control of three-phase active rectifiers by using multiple switching tables. Proceedings of the International Conference of Renewable Energies and Power Quality (ICREPQ'10). Granada, Spain, 1147-1152.
7. Huang, J.; Zhang, A.; Zhang, H.; and Wang, J. (2011). A novel fuzzy-based and voltage-oriented direct power control strategy for rectifier. *Proceedings of the 37th Annual Conference on IEEE Industrial Electronics Society*. Melbourne, Australia, 1115-1119.
8. Blasko, V.; and Kaura, V. (1997). A new mathematical model and control of a three-phase AC-DC voltage source converter. *IEEE Transactions on Power Electronics*, 12(1), 116-123.
9. Malinowski, M.; Kazmierkowski, M.P.; and Trzynadlowski, A.M. (2003). A comparative study of control techniques for PWM rectifiers in AC adjustable speed drives. *IEEE Transactions on Power Electronics*, 18(6), 1390-1396.
10. Ambade, A.P.; Premakumar, S.; Patel, R.; Chaudhari, H.B.; Tillu, A.; Yerge, U.; Rajan, R.N.; and Bakhtsingh, R.I. (2016). Direct power control PWM rectifier using switching table for series resonant converter capacitor charging pulsed power supply. *Proceedings of the IEEE International Conference on Recent Trends in Electronics, Information & Communication Technology* . Bangalore, India, 758-762.
11. Razali, A.M.; Rahman, M.A.; and Rahim, N.A. (2014). Real-time implementation of d-q control for grid connected three phase voltage source converter. *Proceedings of the 40th Annual Conference on IEEE* in *Industrial Electronics Society (IECON)*, Dallas, United States of America, 1733-1739.
12. Fekik, A.; Denoun, H.; Benamrouche, N.; Benyahia, N.; Badji, A.; and Zaouia, M. (2016). Comparative analysis of direct power control and direct power control with space vector modulation of PWM rectifier. *Proceedings of the 4th International Conference in Control Engineering & Information Technology (CEIT)*. Hammamet, Tunisia, 1-6.
13. Zhang, Y.; Peng, Y.; and Qu, C. (2016). Model predictive control and direct power control for PWM rectifiers with active power ripple minimization. *IEEE Transactions on Industry Applications*, 52(6), 4909-4918.

14. Zhang, Y.; Peng, Y.; and Yang, H. (2016). Performance improvement of two-vectors-based model predictive control of PWM rectifier. *IEEE Transactions on Power Electronics,* 31(8), 6016-6030.
15. Zhang, Y.; Qu, C.; Li, Z.; and Zhang, Y. (2013). Mechanism analysis and experimental study of table-based direct power control. *Proceedings of the International Conference in Electrical Machines and Systems (ICEMS).* Busan, South Korea, 2213-2218.
16. Ohnishi, T. (1991). Three phase PWM converter/inverter by means of Instantaneous active and reactive power control. *Proceedings of the International Conference in Industrial Electronics, Control and Instrumentation. Kobe, Japan,* 819-824.
17. Razali, A.M.; and Rahman, M.A. (2011). Performance analysis of three-phase PWM rectifier using direct power control. *Proceedings of the IEEE International Conference in Electric Machines & Drives Conference (IEMDC).* Niagara Falls, Canada, 1603-1608.
18. Bouafia, A.; Krim, F.; and Gaubert, J.-P. (2008). Direct power control of three-phase PWM rectifier based on fuzzy logic controller. *Proceedings of the IEEE International Symposium on Industrial Electronics. Cambridge, United Kingdom,* 323-328.
19. Lamterkati, J.; Khaffalah, M.; Ouboubker, L.; and El-Afia, A. (2016). Fuzzy logic based improved direct power control of three-phase PWM rectifier. *Proceedings of the International Conference* in *Electrical and Information Technologies (ICEIT),* , Tangiers, Morocco, 125-130.
20. Baktash, A.; Vahedi, A.; and Masoum, M.A.S. (2007). Improved switching table for direct power control of three-phase PWM rectifier. *Proceedings of the Australasian Universities Power Engineering Conference*. Perth, Australia, 1-5.
21. Noguchi, T.; Tomiki, H.; Kondo, S.; and Takahashi, I (1998). Direct power control of PWM converter without power-source voltage sensors. *IEEE Transactions on Industry Applications,* 34(3), 473-479.
22. Bouafia, A.; Gaubert, J.-P.; and Krim, F. (2008). Analysis and design of new switching table for direct power control of three-phase PWM rectifier. *Proceedings of the 13th International Power Electronics and Motion Control Conference. Poznan, Poland,* 703-709.
23. Alonso-Martínez, J.; Carrasco, J.E.-G., and S. Arnaltes (2010), Table-based direct power control: A critical review for microgrid applications. *IEEE Transactions on Power Electronics,* 25(12), 2949-2961.
24. Hartani, K.; and Miloud, Y. (2010). Control strategy for three phase voltage source PWM rectifier based on the space vector modulation. *Advances in Electrical and Computer Engineering,* 10(3), 61-65.
25. Dalessandro, L.; Round, S.D.; and Kolar, J.W. (2008). Center-point voltage balancing of hysteresis current controlled three-level PWM rectifiers. *IEEE Transactions on Power Electronics,* 23(5), 2477-2488.
26. Zhang, Y.; Gao, J.; and Qu, C. (2017). Relationship between two direct power control methods for PWM rectifiers under unbalanced network. *IEEE Transactions on Power Electronics,* 32(5), 4084-4094.
27. Zhang, Y.; Liu, J.; and Gao, J. (2017). Direct power control of PWM rectifier under unbalanced network using extended power theory. *Proceedings of the*

IEEE Energy Conversion Congress and Exposition (ECCE). Cincinnati, United States of America, 4617-4621.

28. Zhou, H.; Zha, X.; Jiang, Y.; and Hu, W. (2014). A novel switching table for direct power control of three-phase PWM rectifier. *Proceedings of the International Power Electronics and Application Conference and Exposition (PEAC). Shanghai, China*, 858-863.
29. Gong, B.; Wang, K.; Zhang, J.; You, J.; Luo, Y.; and Wenyi, Z. (2014). Advanced switching table for direct power control of a three-phase PWM rectifier. *Proceedings of the IEEE Conference and Expo Transportation Electrification Asia-Pacific (ITEC Asia-Pacific).* Beijing, China, 1-5.